Research article

JGS
Journal of the Geological Society

Published online February 22, 2018

https://doi.org/10.1144/jgs2017-121 | Vol. 175 | 2018 | pp. 667–678

Geochronological and geochemical constraints on the coexistent N-MORB- and SSZ-type ophiolites in Babu area (SW China) and tectonic implications

Huichuan Liu[1,2]*, Touping Peng[3,4] & Xiaofei Guo[5]

[1] School of Earth Sciences and Engineering, Sun Yat-Sen University, Guangzhou 510275, China
[2] Guangdong Provincial Key Lab of Geodynamics and Geohazards, School of Earth Sciences and Engineering, Sun Yat-sen University, Guangzhou 510275, China
[3] State Key Laboratory of Isotope Geochemistry, Guangzhou Institute of Geochemistry, Chinese Academy of Sciences, Guangzhou 510640, China
[4] CAS Center for Excellence in Tibetan Plateau Earth Sciences, Beijing 100101, China
[5] Faculty of Resource and Environmental Engineering, Jiangxi University of Science and Technology, Ganzhou, Jiangxi, China
H.L., 0000-0002-8203-1382
* Correspondence: liuhuichuan1986@126.com

Abstract: Our detailed geological, geochemical and geochronological investigations indicate the coexistence of late Paleozoic (270–265 Ma) normal middle ocean ridge basalt (N-MORB)-type and suprasubduction-zone (SSZ)-type ophiolites in the Babu area (SW China). Metaperidotite samples from the Babu ophiolites show high Os concentrations and low Re/Os, $^{187}Os/^{188}Os$ and $^{187}Re/^{188}Os$ ratios, and represent residual upper mantle. Metagabbro and metabasalt samples show light rare earth element (LREE)-depleted REE patterns and N-MORB-like primitive mantle-normalized spider diagrams without Nb–Ta and Zr–Hf anomalies, and depleted Sr–Nd isotopic compositions ($\varepsilon_{Nd}(t) = +6.9 – +8.3$). These geochemical and Re–Os–Sr–Nd isotopic data show that the Babu ophiolites are derived from a depleted mantle source and represent ancient N-MORB-like oceanic crust. In addition, peridotites, basalts and boninites with SSZ signatures (e.g. Nb–Ta negative anomalies) were also reported in the Babu ophiolites consistent with their generation in a forearc or arc setting. In combination with the arc-related high-$Mg^{\#}$ limburgite, basalt and andesite, these late Paleozoic ultramafic–mafic rocks are genetically related to Paleotethyan subduction, rather than being Emeishan mantle plume related. The coexisting N-MORB- and SSZ-type ophiolites in the Babu area show similar geochemical and geochronological characteristics to the Jinshajiang–Ailaoshan–Song Ma ophiolites.

Supplementary material: A description of the geology of the Babu ultramafic–mafic complex, sample descriptions, detailed analytical methods and results, and a summary of previously published age data for late Paleozoic magmatic rocks along the China–Vietnam border are available at https://doi.org/10.6084/m9.figshare.c.4007569

Received 12 October 2017; **revised** 22 December 2017; **accepted** 18 January 2018

During the late Paleozoic to early Mesozoic, a significant Paleotethyan ocean extended from the Alps through Afghanistan and southwestern China to Peninsular Malaysia (Yin & Harrison 2000; Metcalfe 2011; Zi *et al.* 2012; Zaw *et al.* 2014; Zhang *et al.* 2016). In SE Asia, the Paleotethyan ocean and/or back-arc basins developed along the Bentong–Raub–Chiang Mai–Changning–Menglian suture and Jinshajiang–Ailaoshan–Song Ma suture, which separate the Simao–Indochina block from the Sibumasu block to the west and South China block to the east, respectively (Fig. 1a; Wang *et al.* 2000*a*; Sone & Metcalfe 2008; Jian *et al.* 2009*a*,*b*; Fan *et al.* 2010; Metcalfe 2011; Hara *et al.* 2012; Lai *et al.* 2014*a*). However, the exact location of the southeastern extension of the Jinshajiang–Ailaoshan–Song Ma suture (i.e. the boundary between the Simao–Indochina and South China blocks) is still highly disputed. Different locations, including the Song Ma belt (Trung *et al.* 2006; Zhang *et al.* 2013*b*; Ngo *et al.* 2016), the Song Da fault (Sengor & Hsu 1984), the Dien Bien fault (Roger *et al.* 2014), the Dian–Qiong belt (Cai & Zhang 2009) and the Truong Son belt (Usuki *et al.* 2013; Shi *et al.* 2015), have been reported in the literature. Along the Jinshajiang–Ailaoshan–Song Ma suture, previous work has been focused more commonly on the Jinshajiang (Wang *et al.* 2000*b*; Jian *et al.* 2008; Zi *et al.* 2012), Ailaoshan (Wang *et al.* 2000*a*; Jian *et al.* 2009*b*; Lai *et al.* 2014*a*,*b*) and Song Ma igneous belts (Zhang *et al.* 2013*b*, 2014; Ngo *et al.* 2016), but much less attention has been paid to the late Paleozoic ultramafic–mafic rocks in the adjacent area of SW China and NE Vietnam (Fig. 1b). Different perspectives have been proposed for their petrogenesis as (1) a part of the Emeishan large igneous province (Hanski *et al.* 2010; Li *et al.* 2016), (2) an expression of the Song Da rift (Polyakov *et al.* 1998; Balykin *et al.* 2010), (3) dismembered ophiolites formed in an arc and/or back-arc oceanic basin (Thanh *et al.* 2014), or (4) relics of the Paleotethyan oceanic crust and arc magmatic rocks (Wu *et al.* 1999). This pending problem not only hampers our understanding of the spatial and temporal distributions of the Jinshajiang–Ailaoshan–Song Ma Paleotethyan branch ocean and/or back-arc basin, but also results in controversy on its closure processes (Lan *et al.* 2003; Lepvrier *et al.* 2004; Zi *et al.* 2012; Faure *et al.* 2014; Liu *et al.* 2015).

The main reason for this controversy is the lack of systematical geological studies on the late Paleozoic ultramafic–mafic rocks in the adjacent area of China and Vietnam. We carried out field investigations and new zircon U–Pb geochronological, whole-rock elemental and Sr–Nd–Re–Os isotopic analyses on the metaperidotite, metagabbro and metabasalt from the Babu area (NE Yunnan province, China; Fig. 2). Our observations show the coexistence of Permian (265–270 Ma) normal middle ocean ridge basalt

© 2018 The Author(s). Published by The Geological Society of London. All rights reserved. For permissions: http://www.geolsoc.org.uk/permissions.
Publishing disclaimer: www.geolsoc.org.uk/pub_ethics

Downloaded from https://pubs.geoscienceworld.org/jgs/article-pdf/175/4/667/4240757/jgs2017-121.pdf
by Guangzhou Institute of Geochemistry CAS user

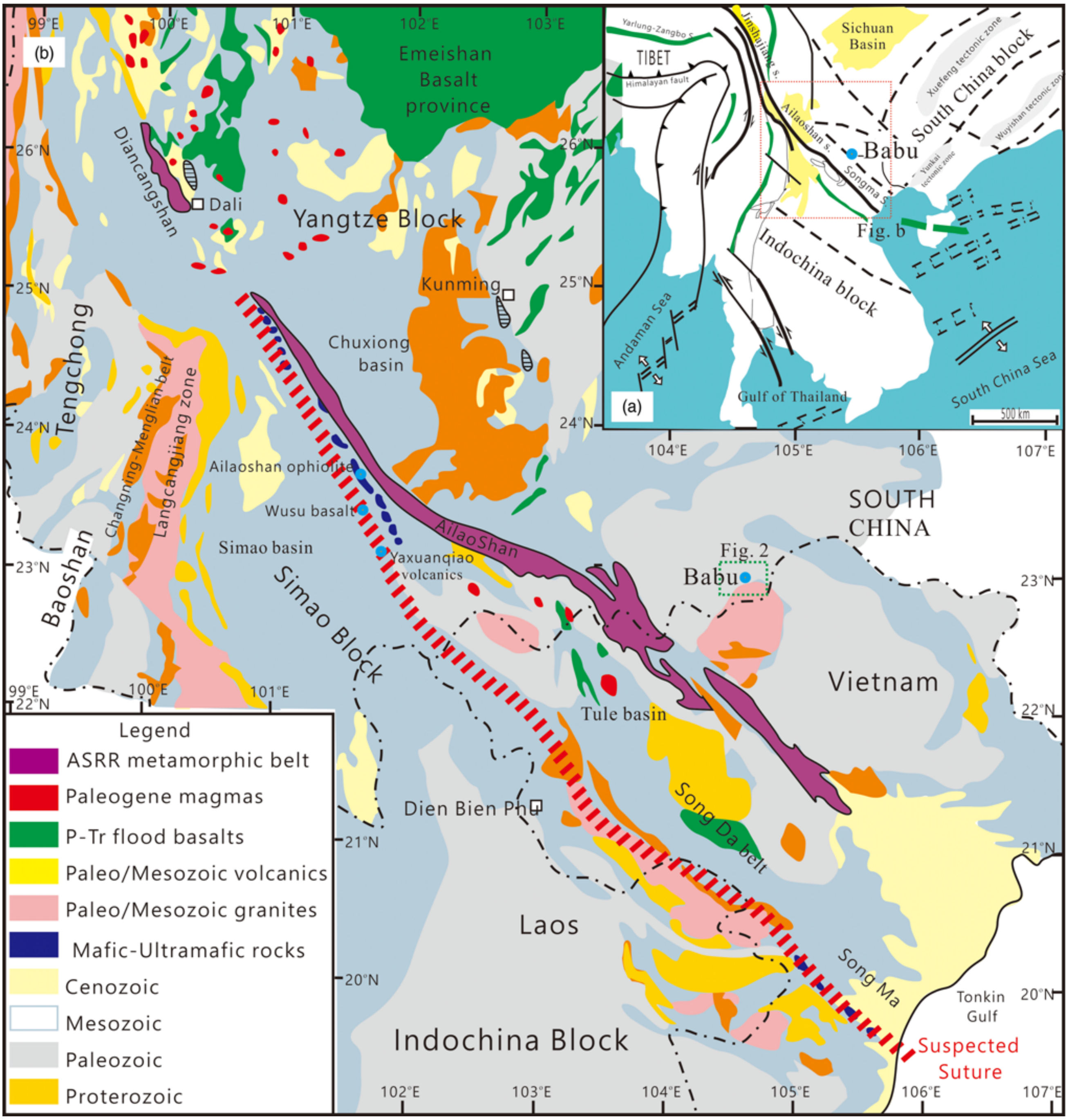

Fig. 1. (**a**) Tectonic outline of SE Asia (Wang *et al.* 2013) and (**b**) sketch structural map of the adjacent region between South China, Indochina, Simao and Sibumasu, showing the main tectonic units and sutures (modified from Fan *et al.* 2010). ASRR, Ailaoshan–Red River.

(N-MORB)-type and suprasubduction-zone (SSZ)-type ophiolites in the Babu area. Ophiolites represent fragments of upper mantle and oceanic crust, and play an important role in identifying the suture zone and unveiling the evolutionary history of fossil ocean and/or back-arc basins (Dilek *et al.* 2008; Zhang *et al.* 2008; Dilek & Furnes 2011). Thus, these data, together with neighbouring back-arc or arc igneous rocks, allow us to investigate the spatial and temporal distributions of the Jinshajiang–Ailaoshan–Song Ma suture.

Regional geological background

SE Asia is composed of four major tectonic blocks: West Burma, Sibumasu, Indochina and South China (Fig. 1a). West Burma is separated from Sibumasu by a Meso-Tethys suture stretching along the Shan Boundary Fault (Deng *et al.* 2014*a*). The Changning–Menglian–Inthanon suture lies between the Sibumasu and West Simao–Indochina blocks (Metcalfe 2002, 2011). East of the Changning–Menglian–Inthanon suture are the Simao–Indochina and South China blocks, which are separated by the Jinshajiang–Ailaoshan–Song Ma suture (Faure *et al.* 2014; Xia *et al.* 2016). The oldest rocks of the Simao–Indochina block are represented by the *c.* 2.9 Ga (zircon U–Pb age) protolith of the orthogneiss complex in northern Vietnam (Nam *et al.* 2003). Lower Paleozoic sequences of the Simao–Indochina block are unconformably overlain by Middle Devonian basal conglomerates and shallow-marine sedimentary rocks and/or Carboniferous to Permian shallow-marine, paralic and continental successions (Metcalfe 2006). The upper Paleozoic sequence is unconformably overlain by the upper Triassic Gaoshanzhai and Waiguchun Formations (Yunnan BGMR 1990). The western margin of the South China block consists of Archean to

Downloaded from https://pubs.geoscienceworld.org/jgs/article-pdf/175/4/667/4240757/jgs2017-121.pdf
by Guangzhou Institute of Geochemistry CAS user

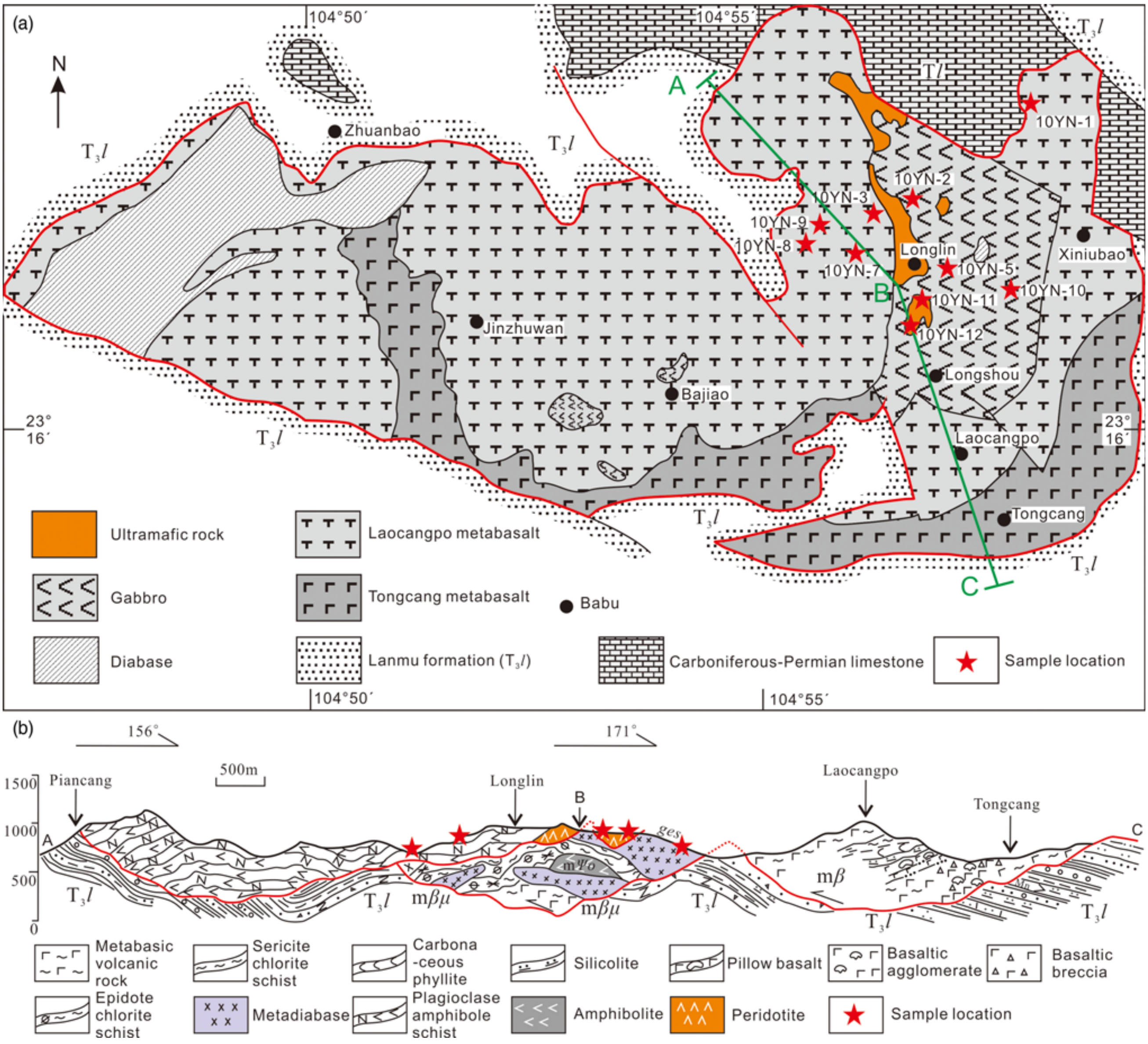

Fig. 2. (**a**) Geological map showing the stratigraphic and igneous components of the Babu area (modified from Xu *et al.* 2008*a*). (**b**) Cross-section of the Babu ophiolites (modified from Zhang *et al.* 2013*a*).

Paleoproterozoic crystalline basement and Neoproterozoic to lower Paleozoic and upper Paleozoic marine assemblages (Cawood *et al.* 2013; Wang *et al.* 2013). Approximately 260 Ma Emeishan continental flood basalts, Triassic limestones and fine-grained clastic rocks, and Late Mesozoic terrestrial red beds overlie the pre-Triassic stratum (Zhang *et al.* 2006; Lepvrier *et al.* 2008; Deng *et al.* 2014*b*; Li *et al.* 2016).

Neoproterozoic volcanic arc rocks in the western margin of the South China block indicate that the amalgamation of the South China and Simao–Indochina blocks occurred in the Mid-Neoproterozoic (860–730 Ma; Cai *et al.* 2014, 2015; Qi *et al.* 2014; Wang *et al.* 2016). The Proterozoic metamorphic rocks, pre-Early Devonian sedimentary cover and Middle Devonian conglomerate in the Simao–Indochina block lithologically resemble those of the South China block and suggest a Cambrian–Silurian linkage between the two blocks (Yunnan BGMR 1990; Zhong 1998; Faure *et al.* 2014; Wang *et al.* 2014*b*; Xia *et al.* 2016). The existence of Silurian rift-related amphibolite xenoliths (439–404 Ma) in the Jinshajiang ophiolitic rocks indicates that the South China–Indochina initial break-up may be traced to Early Silurian times (Jian *et al.* 2009*b*). Then a branch ocean or back-arc basin along the Jinshajiang–Ailaoshan–Song Ma suture slowly spread and commenced its closure after reaching its maximum expansion (Jian *et al.* 2009*a*,*b*; Fan *et al.* 2010; Zi *et al.* 2012; Liu *et al.* 2014, 2015, 2017*a*,*b*).

A description of the geology of the Babu ultramafic–mafic complex and sample descriptions are given in the supplementary material. In this study, we collected serpentinite, diabasic–gabbroic amphibolite and greenschist samples from the Babu complex for *in situ* U–Pb dating and geochemical analyses. Detailed analytical methods and results are given in the supplementary material.

Analytical results

Geochronology

To determine the formation age of the Babu ophiolite, samples 10YN-01 (metabasalt) and 10YN-10 (metagabbro) were selected for secondary ionization mass spectrometry (SIMS) zircon U–Pb dating (Fig. 3). Cathodoluminescence (CL) imaging reveals that all zircon grains from the gabbro and basalt samples are transparent or translucent with a minority displaying a green tinge along grain boundaries. They are typically subhedral and fragmentary (Fig. 3b and d) and are very similar in terms of morphology and zonation to

Downloaded from https://pubs.geoscienceworld.org/jgs/article-pdf/175/4/667/4240757/jgs2017-121.pdf
by Guangzhou Institute of Geochemistry CAS user

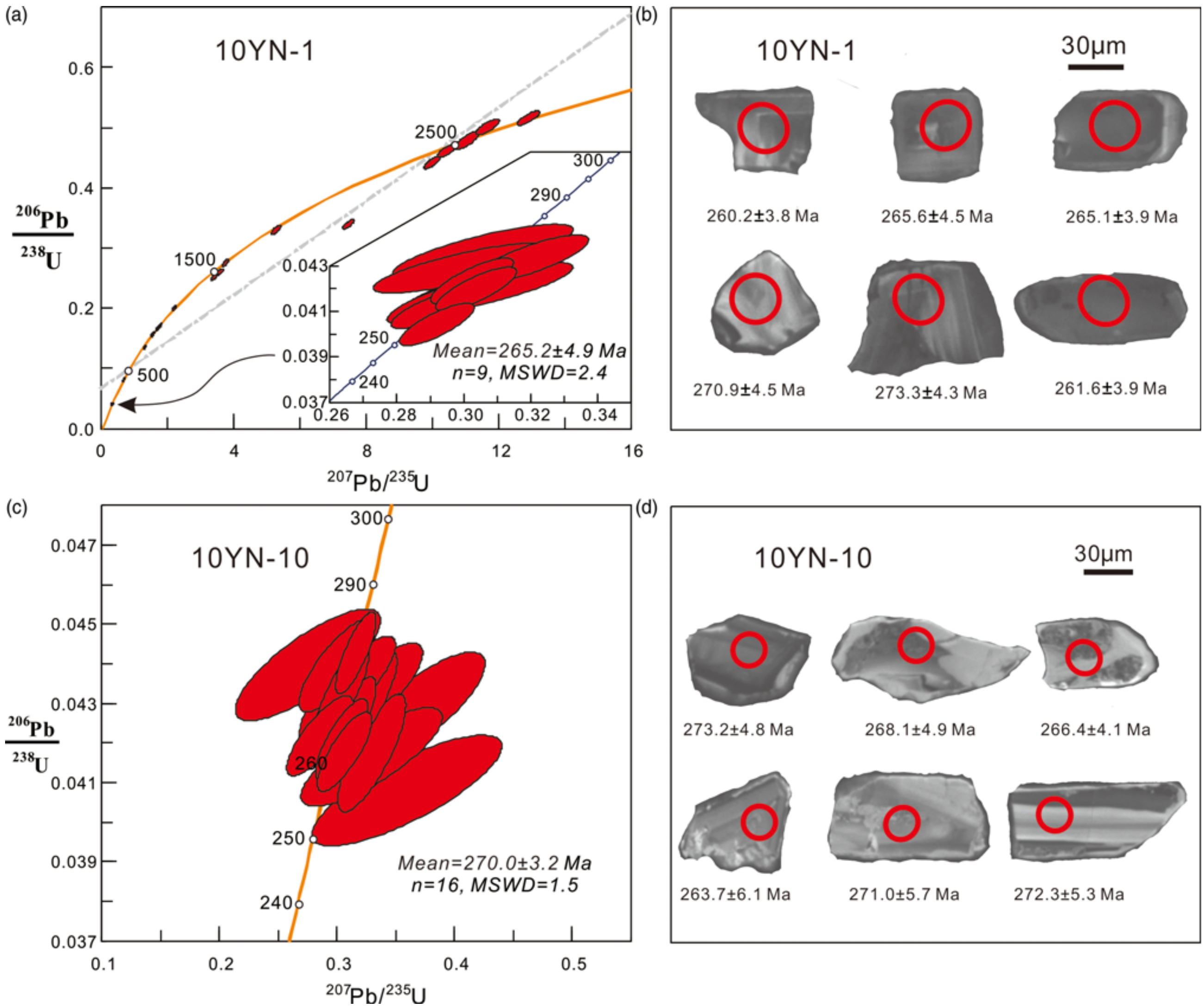

Fig. 3. SIMS zircon U–Pb concordia diagrams for the metabasalt (**a**; 10YN-01) and metagabbro (**c**; 10YN-10). Cathodoluminescence (CL) images of representative zircon grains (**b**, **d**). Red circles on CL images mark analytical site on each grain.

the zircons separated from a diabase sample of the Ailaoshan ophiolite (Jian *et al.* 2009*b*). Most of the zircons contain well-defined, broad sector zones, which become thinner from core to rim. Cores are dark, indicating a high U concentration relative to rims, which is verified by Figure 3 (Whattam *et al.* 2006). These backscatter electron (BSE) and CL images show typical features of igneous zircon (Hanchar & Watson 2003). Zircon U–Pb dating results are presented on concordia plots in Figure 3.

Thirty analyses were performed on 30 zircons from sample 10YN-01. Twenty-one of them are inherited grains, with $^{206}Pb/^{238}U$ apparent ages ranging from 505 to 2655 Ma. These crustally derived zircons may have been introduced into the metabasalts after obduction via microscopic melt networks, as happened in the Tumut ophiolitic mélange of the Lachlan fold belt (southeastern Australia; e.g. Belousova *et al.* 2015). The remaining nine spots have Th/U ratios varying from 0.36 to 0.94, consistent with an igneous origin (Wu & Zheng 2004), and yield a weighted mean $^{206}Pb/^{238}U$ age of 265 ± 5 Ma (MSWD = 2.4, Fig. 3a).

Sixteen analyses were performed on 16 zircon grains from sample 10YN-10. These analyses document Th/U ratios ranging from 0.18 to 2.40, consistent with an igneous origin (Wu & Zheng 2004). Cores, rims, and high and low U concentration regions all yield the same age within the uncertainties. They yield $^{206}Pb/^{238}U$ apparent ages ranging from 258 to 279 Ma, with a weighted mean $^{206}Pb/^{238}U$ age of 270 ± 3 Ma ($n = 16$, MSWD = 1.5, Fig. 3c).

Geochemical characteristics

We carried out major and trace elemental, and Sr–Nd isotopic analyses for the metabasalt, metagabbro and metaperidotite samples, and Re–Os isotopic analyses for the metaperidotite samples. The whole-rock major oxide data for the studied samples are given in Figure 4, the Re–Os isotopic data in Figure 5, and the whole-rock trace element data in Figure 6. The initial Sr–Nd isotopic ratios were recalculated to their crystallization ages of 265–270 Ma and the results are given in Figure 7.

Metaperidotite

The protolith of our metaperidotite samples is mainly harzburgite and pyroxenite. They show low SiO_2 (38.7–40.1 wt%), TiO_2 (*c.* 0.01 wt%), Al_2O_3 (0.89–1.34 wt%), CaO (0.05–1.39 wt%), K_2O (0.01 wt%) and Na_2O (<0.1 wt%) contents, and extremely high MgO (37.6–38.5 wt%) content. The metaperidotites have variable incompatible element contents, and exhibit U-type chrondrite-normalized rare earth element (REE) patterns and random primitive mantle-normalized spider diagrams (Fig. 6). In studying formation of the ultramafic–mafic complex, one of our concerns is how to distinguish the residual mantle rocks from partial melts of primary mantle (Saal *et al.* 2001; Gao *et al.* 2002; Shi *et al.* 2012*b*; Uysal *et al.* 2012). During melting processes of the upper

Downloaded from https://pubs.geoscienceworld.org/jgs/article-pdf/175/4/667/4240757/jgs2017-121.pdf
by Guangzhou Institute of Geochemistry CAS user

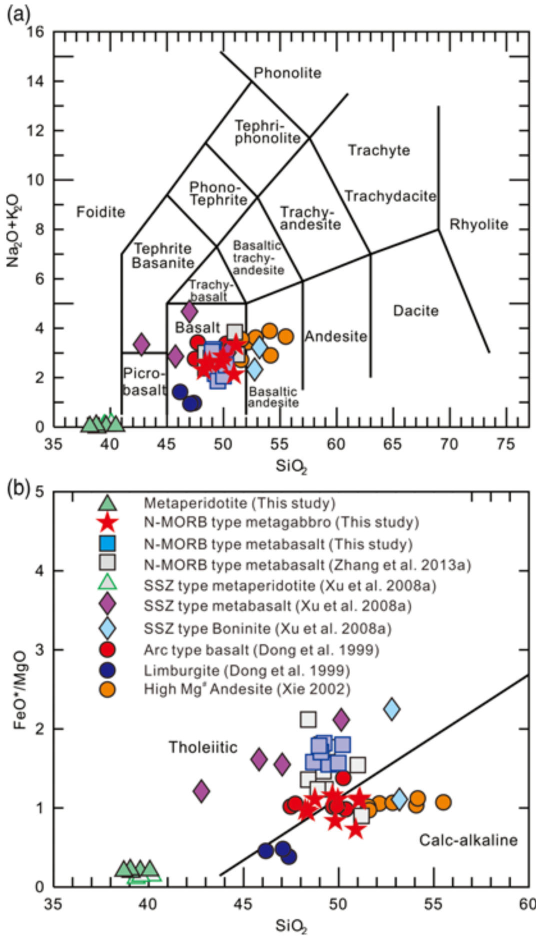

Fig. 4. (**a**) SiO_2–$K_2O + Na_2O$ plot (Le Bas *et al.* 1986); (**b**) FeO_T/MgO v. SiO_2 diagram distinguishing tholeiitic and calc-alkaline series (Miyashiro 1974).

mantle, in lithophile isotopic systems such as Rb–Sr, Sm–Nd and U–Pb both elements are incompatible, and will not become fractionated (Shi *et al.* 2012*b*); thus they cannot be used to trace the upper mantle melting processes. However, the Re–Os isotope system is different. Os behaves as a highly compatible element whereas the more incompatible Re is partitioned into the melt, and Re and Os have both chalcophile and siderophile affinities (Shirey & Walker 1998; Saal *et al.* 2001; Shi *et al.* 2012*a*). Consequently, residual mantle rocks have higher Os concentrations and lower Re/Os, $^{187}Os/^{188}Os$ and $^{187}Re/^{188}Os$ ratios than the melts (Fig. 5). Also, the Re–Os isotope system is generally considered to be more resistant to late metasomatic disturbances than the Rb–Sr, Sm–Nd and U–Pb isotopic systems (Luck & Allègre 1991; Roy-Barman *et al.* 1996; Burton *et al.* 1999). To investigate the residual mantle rocks and partial melts of the Babu ultramafic–mafic complex, we carried out Re–Os isotopic analyses for the metaperidotite samples. Our samples show high Os concentrations and lower Re/Os, $^{187}Os/^{188}Os$ and $^{187}Re/^{188}Os$ ratios, and represent residual upper mantle (Fig. 5).

Metagabbro

The metagabbro samples show $Al_2O_3 = 12.50$–16.24 wt%, $CaO = 10.76$–14.37 wt% and $Na_2O = 2.11$–3.28 wt%, and plot in the gabbro field in the total alkalis v. silica (TAS) diagram with calc-alkaline geochemical compositions (Fig. 4). They show LREE-depleted REE patterns ($(La/Sm)_{CN} = 0.30$–0.55, $(La/Yb)_{CN} = 0.29$–0.66), suggesting an N-MORB-type affinity. This is further confirmed by the N-MORB-like primitive mantle-normalized spider diagrams without negative Nb, Ta, Zr or Hf anomalies (Fig. 6). These mafic rocks display Nb/La ratios of 0.17–0.34 (≤1), Hf/Ta ratios of 21.17–28.93 (>5), La/Ta ratios of 23.87–34.05 (>15), Ti/Y ratios of 177.66–291.38 (<350), Ti/V of 14.14–30.71 (<30), Ta contents of 0.03–0.08 ppm (<0.7 ppm) and Nb contents of 0.11–0.72 ppm (≤12 ppm). Furthermore, they show depleted Sr–Nd isotopic compositions, with $(^{87}Sr/^{86}Sr)_i = 0.70346$–$0.70563$ and $\varepsilon_{Nd}(t) = +6.9$ – $+8.3$ (Fig. 7). These geochemical characters resemble those of typical N-MORB (Sun & McDonough 1989; Dilek *et al.* 2008).

Metabasalt

The metabasalt samples from the Babu ophiolite show $Al_2O_3 = 2.36$–13.31 wt%, $CaO = 9.40$–11.26 wt%, $Na_2O = 1.79$–3.08 wt% and $Na_2O/K_2O = 19.8$–43.6, and plot in the basalt field in the TAS diagram (Fig. 4). These samples define a typical tholeiite compositional trend in SiO_2–FeO_T/MgO diagrams. They are depleted in highly incompatible elements and LREE, and show left-leaning smooth primitive mantle-normalized spider and chondrite-normalized REE diagrams ($(La/Sm)_{CN} = 0.53$–0.61, $(La/Yb)_{CN} = 0.54$–0.62; Fig. 6). These mafic rocks display Nb/La ratios of 0.41–0.45 (≤1), Hf/Ta ratios of 18.08–22.96 (>5), La/Ta ratios of 22.91–27.54 (>15), Ti/Y ratios of 200.58–263.13 (<350), Ti/V ratios of 21.40–24.40 (<30), Ta contents of 0.12–0.16 ppm (<0.7 ppm) and Nb contents of 1.27–1.77 ppm (≤12 ppm). The

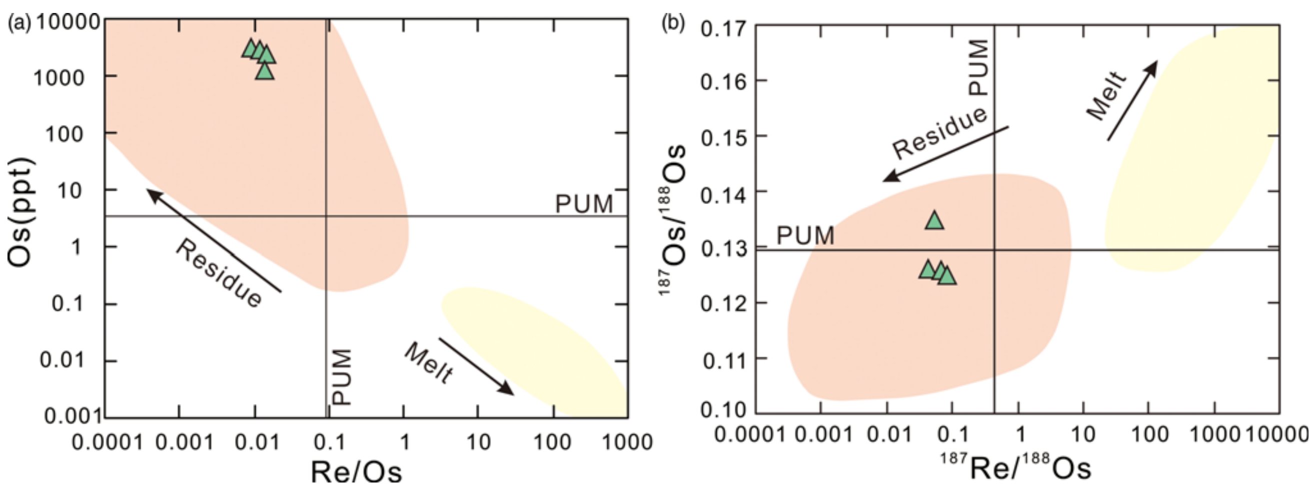

Fig. 5. Re–Os isotopic compositions of the metaperidotite from the Babu area. The data for the primary upper mantle (PUM) and the trend for the residue and melt are from Shi *et al.* (2006).

Downloaded from https://pubs.geoscienceworld.org/jgs/article-pdf/175/4/667/4240757/jgs2017-121.pdf
by Guangzhou Institute of Geochemistry CAS user

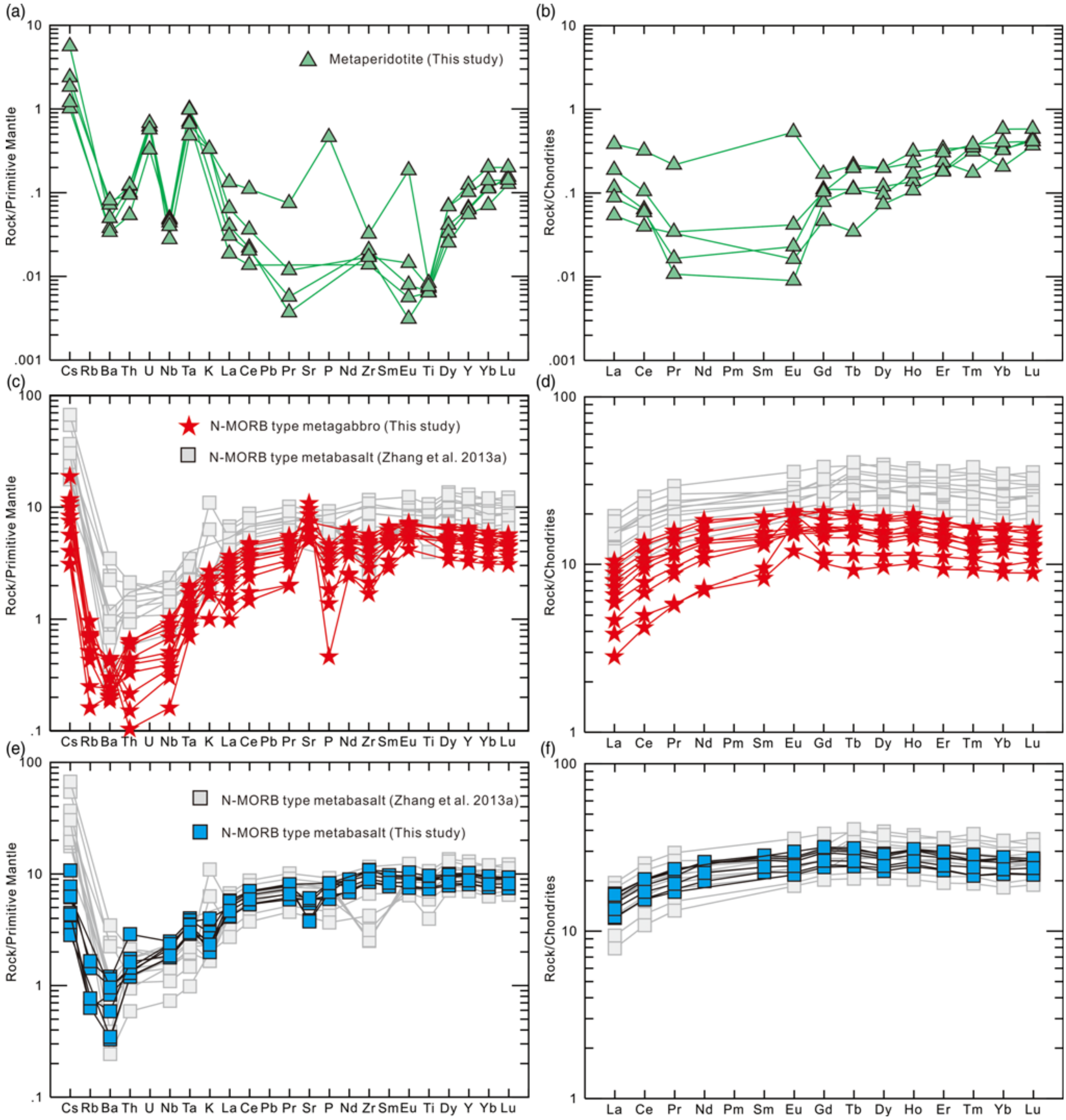

Fig. 6. Primitive mantle-normalized incompatible elemental spidergrams and chondrite-normalized REE patterns for the metaperidotite (**a**, **b**), metagabbro (**c**, **d**) and metabasalt samples (**e**, **f**) in this study. N-MORB data from Zhang *et al.* (2013*a*) are shown for comparison. Normalized values for primitive mantle and chondrite are from Sun & McDonough (1989).

metabasalt samples have similar depleted Sr–Nd isotopic compositions to the Babu gabbros, with $(^{87}Sr/^{86}Sr)_i = 0.70330–0.70494$ and $\varepsilon_{Nd}(t) = +7.5 – +8.0$ (Fig. 7). These geochemical characters also resemble those of typical N-MORB (Sun & McDonough 1989; Dilek *et al.* 2008).

Coexistent N-MORB- and SSZ-type ophiolites in the Babu area

Faure *et al.* (2014) argued that the Babu ultramafic–mafic rocks are not ophiolites, but intraplate basalts related to the Emeishan plume. The voluminous Emeishan large igneous province activity in southwestern China is generally considered to occur in a short interval between 260 and 257 Ma (Xu *et al.* 2001, 2008*b*; Wang *et al.* 2012). However, Wu *et al.* (1999) reported a Sm–Nd isochronal age of 328 ± 9 Ma for the basalt of the Babu ultramafic–mafic complex. Recently, Zhang *et al.* (2013*a*) proposed a zircon U–Pb age of 272 ± 8 Ma for the metagabbro from the Babu complex. Du *et al.* (2014) obtained a zircon U–Pb age of 359 ± 6 Ma for the metabasalt. Our dating results (265–270 Ma) are consistent with these zircon U–Pb ages, and more accurate. The 359–265 Ma age represents the formation age of the Babu ultramafic–mafic complex. Thus, the Babu ultramafic–mafic complex is significantly older than the Emeishan large igneous province activity, and cannot be related to the Emeishan plume. In the Penrose definition (e.g. Dilek & Furnes 2014, and references therein), ophiolite is described as a 'distinctive assemblage of mafic to ultramafic rocks' that includes, from bottom to top, tectonized

Downloaded from https://pubs.geoscienceworld.org/jgs/article-pdf/175/4/667/4240757/jgs2017-121.pdf
by Guangzhou Institute of Geochemistry CAS user

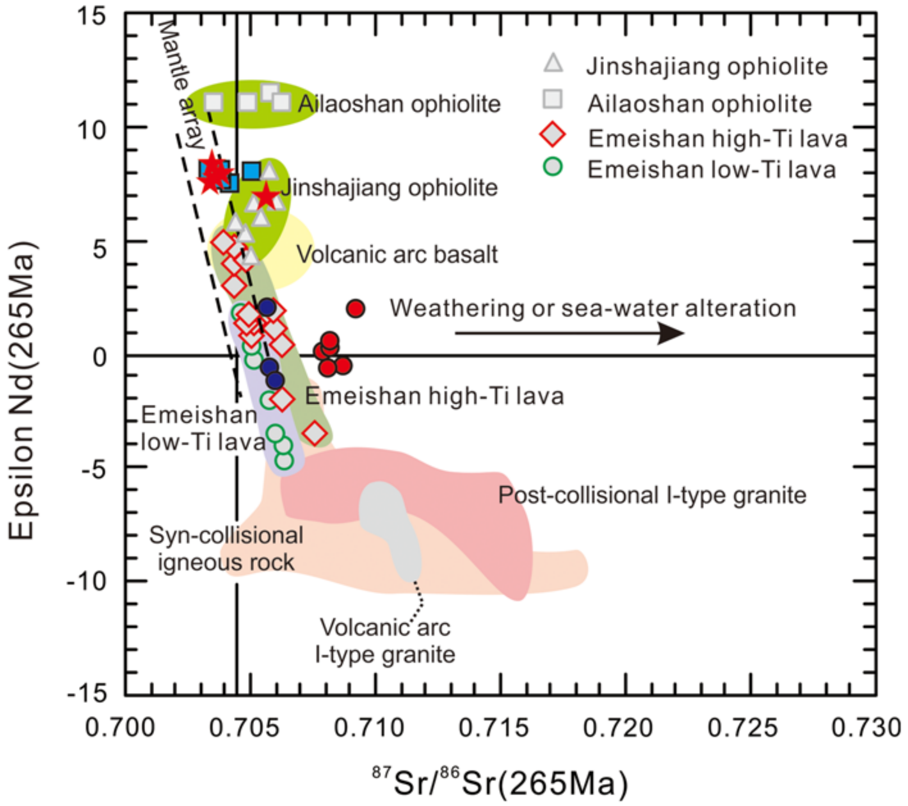

Fig. 7. $^{87}Sr/^{86}Sr(t)$ v. $\varepsilon_{Nd}(t)$ diagram. Data for the Ailaoshan and Jinshajiang ophiolites are from Xu & Castillo (2004). Data for the volcanic arc basalt are from Fan *et al.* (2010) and Liu *et al.* (2017*b*). Data for Emeishan high-Ti and low-Ti lavas are from Xu *et al.* (2001). Data for volcanic arc I-type granite are from Zi *et al.* (2013) and Liu *et al.* (2015). Data for syn-collisional igneous rock are from Zi *et al.* (2013) and Liu *et al.* (2015). Data for post-collisional igneous rock are from Zhu *et al.* (2011). Symbols for the Jinshajiang ophiolite, Ailaoshan ophiolite, Eimeishan high-Ti and low-Ti lavas are shown in the figure; other symbols are the same as in Figure 4.

peridotites, cumulate peridotites, and pyroxenites overlain by layered gabbros, sheeted basaltic dykes, a volcanic sequence and a sedimentary cover (e.g. Dilek *et al.* 2008; Dilek & Furnes 2011, 2014; Furnes *et al.* 2014, 2015; Pearce 2014; Furnes & Dilek 2017). As shown in Figure 2, the Babu ultramafic–mafic complex is composed of meta-peridotite, diabases–gabbros and mafic lavas. Also, Feng & Liu (2002) reported overlying siliceous rocks with Permian radiolarians. Thus, an alternative plausible scenario based on the geochronology and similar rock associations is that the Babu ultramafic–mafic rocks are ophiolites and represent relics of the late Paleozoic (359–265 Ma) oceanic crust, as proposed by Zhong (1998).

Dilek *et al.* (2008) classified the ophiolites into MORB and SSZ types according to their geochemical affinities to MORB and SSZ basalt, respectively. Thorium (Th) is a key element in distinguishing these two types of ophiolites, because Th is enriched in arc-related lavas and depleted in mid-ocean ridge lavas, and it is immobile during seawater alteration and metamorphism up to the melting temperature (Pearce 2003), in contrast to U, which is mobile in fluids (Hawkesworth *et al.* 1997). Enrichment in Th relative to Nb and Ta is indicative of a suprasubduction-zone setting (e.g. Dilek & Furnes 2014; Pearce 2014; Saccani 2015). Titanium (Ti) is also a key parameter for investigating subduction-influenced ridges (e.g. Pearce 2014).

Our metagabbro samples with no cumulate textures are characterized by relatively high MgO ($Mg^{\#} = 64.5–74.3$), Cr (228–965 ppm) and Ni (74–124 ppm) contents, and could approach frozen liquids of primary magma (Litvak & Poma 2010). They show smooth N-MORB-type primitive mantle-normalized spider diagrams and chondrite-normalized REE patterns (Fig. 6c and d), without Th enrichment. Our metabasalt samples also show typical N-MORB-type trace element compositions. In Figure 8, both the metabasalts and metagabbros plot within the MORB–OIB (ocean island basalt) array (Fig. 8a) and in the field of N-MORB (Fig. 8b and c). Their depleted Sr–Nd isotopic compositions with $\varepsilon_{Nd}(t)$ of +7.5 – +8.0 and +7.9 – +8.3, respectively, also mimic the typical N-MORB (Shinjo *et al.* 2015). These characteristics suggest that our Babu samples have N-MORB features and were mainly derived from an N-MORB-like depleted mantle source.

In the Babu area, Xu *et al.* (2008*a*) reported another type of ultramafic–mafic–intermediate rock association with significant Th enrichment, which possibly represents the SSZ-type ophiolite. Major-element chemistry of the samples allowed us to classify them into peridotite, tholeiite and boninite (Xu *et al.* 2008*a*). The metaperidotites show low and variable incompatible element contents. Unlike our harzburgite and pyroxenite samples, they have high CaO (0.11–1.55 wt%) and Na_2O (0.04–0.12 wt%) contents, and significant large ion lithophile element (LILE) enrichment and Nb–Ta negative anomalies ($Nb^* = 0.17–0.79$) on primitive mantle-normalized spider diagrams. The tholeiites have high FeO_T/MgO ratios and plot in the tholeiite field (Fig. 4b). They show significant LILE enrichment, high field strength element (HFSE) depletion ($Nb^* = 0.19–0.96$) and flat chondrite-normalized REE patterns ($(La/Yb)_n = 0.63–1.75$). The boninites are characterized by high MgO (25.5–28.1 wt%), SiO_2 (52.3–53.1 wt%), Cr (2036–2015 ppm) and Ni (1066–1244 ppm) contents, and low TiO_2 (0.03–0.07 wt%) contents and Zr/Y ratios (0.09–0.39), similar to boninite in modern forearc basins (Macpherson & Hall 2001). The Babu boninites also show low incompatible element contents ($(\text{total REE})_n = 16.5–92.2$), significant LILE enrichment and HFSE depletion ($Nb^* = 0.08–0.09$). In Figure 8, they are displaced from the MORB–OIB array to higher Th/Yb values (Fig. 8a) and plot in the field of island arc tholeiite (IAT; Fig. 8c). These arc-like geochemical features suggest an enriched mantle source and slab subduction-related tectonic setting.

In summary, the N-MORB-type and SSZ-type ophiolites coexist in the Babu area.

Tectonic affinities

A summary of previously published age data for late Paleozoic magmatic rocks along the China–Vietnam border is given in the

Downloaded from https://pubs.geoscienceworld.org/jgs/article-pdf/175/4/667/4240757/jgs2017-121.pdf
by Guangzhou Institute of Geochemistry CAS user

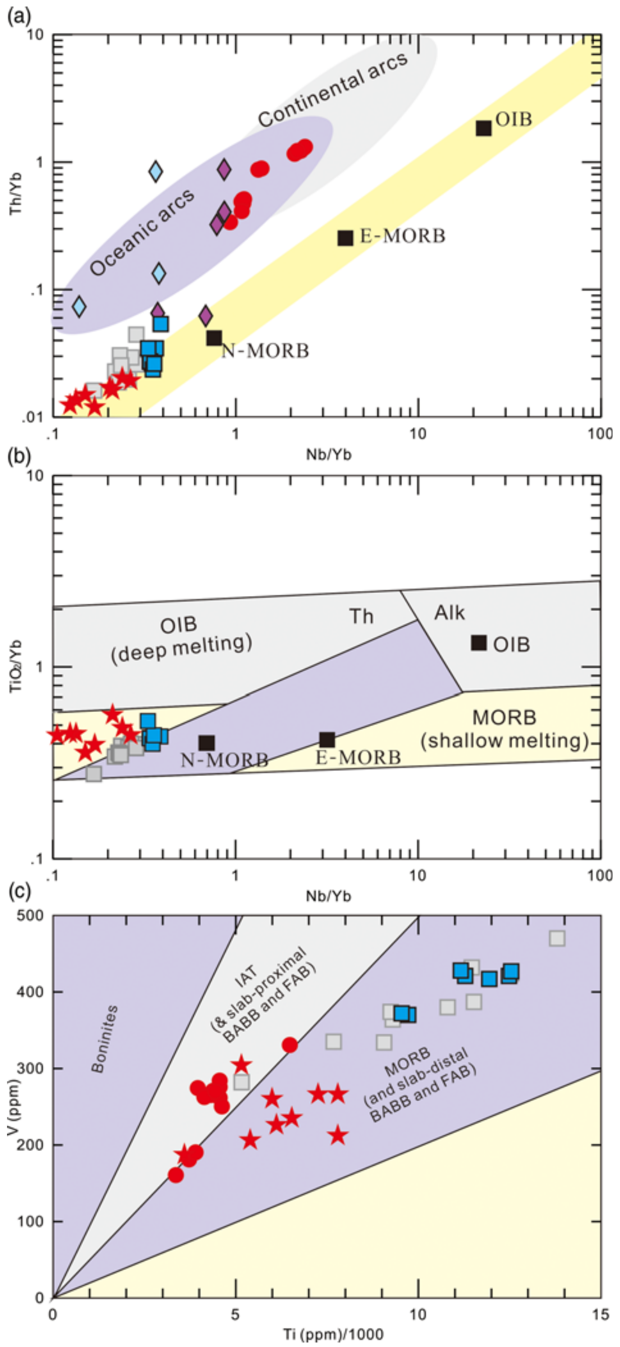

Fig. 8. Tectonic discrimination diagrams (Dilek & Furnes 2011, 2014; Pearce 2014; Furnes *et al.* 2015). Symbols are the same as in Figure 4. E-MORB, enriched mid-ocean ridge basalt; BABB, back-arc basin basalt; FAB, forearc basalt; IAT, island arc tholeiite.

supplementary material. For the petrogenesis of the late Paleozoic ultramafic–mafic rocks in the Babu area, different perspectives have been proposed; they have been considered to be (1) a part of the Emeishan large igneous province (Hanski *et al.* 2010; Li *et al.* 2016), (2) an expression of the Song Da rift (Polyakov *et al.* 1998; Balykin *et al.* 2010), (3) dismembered ophiolites formed in a back-arc oceanic and/or intra-continental basin (Thanh *et al.* 2014), or (4) relics of the Paleotethyan oceanic crust and arc magmatic rocks (Wu *et al.* 1999).

Emeishan large igneous province related rocks were previously reported in four areas: (1) the Song Da zone (including the Tule basin and Phan Si Pan Complex in NE Vietnam and the Jinping area of China; Wang *et al.* 2007; Balykin *et al.* 2010); (2) the Dulong–Song Chay dome (Hoa *et al.* 2008*a*,*b*); (3) the Song Hien domain in NE Vietnam (Hoa *et al.* 2008*a*,*b*); (4) the SW margin of the Youjiang basin (Zhou *et al.* 2006; Fan *et al.* 2008; Huang *et al.* 2014). Areas (2) and (3) (i.e. the Dulong–Song Chay dome and the Song Hien domain) were proposed by Hoa *et al.* (2008*a*,*b*) based on zircon U–Pb ages; no geochemical data have been reported. However, Hanski *et al.* (2010) and Li *et al.* (2016) considered that in northern Vietnam the Emeishan large igneous province related rocks cropped out only in the Song Da area and late Paleozoic magmas in the Dulong–Song Chay dome and the Song Hien domain are not associated with the Emeishan mantle plume. Thanh *et al.* (2014) systematically carried out geochemical studies on the Cao Bang mafic–ultramafic magmas in the Song Hien domain and suggested a back-arc environment for their petrogenesis. Halpin *et al.* (2016) also proposed that the late Paleozoic ultramafic–mafic rocks are not genetically linked to the Emeishan large igneous province, and may correlate with the Jinshajiang–Ailaoshan–Song Ma Paleotethyan branch ocean or back-arc basin. Also, Polyakov *et al.* (1998) and Glotov *et al.* (2001) argued for the development of a late Paleozoic continental rift in the light of the OIB-like komatiite–basalt complex in the Jinping–Song Da area. A recent geochemical study by Tran *et al.* (2015) suggested that these OIB-like komatiite–basalt complexes in the Song Da zone are parts of the Emeishan large igneous province, and that the Song Da rift did not exist.

In addition to the Emeishan large igneous province related rocks, our studies identified coexistent N-MORB- and SSZ-type ophiolites along the China–Vietnam border. The N-MORB ophiolites are relics of oceanic crust and the SSZ-type ophiolites represent arc magmatic rocks. In the nearby Jianshui area, Dong & Zhu (1999) and Xie (2002) reported another Permian mafic–intermediate rock association, which mainly includes subalkaline limburgite, basalt and andesite. The limburgite shows high MgO (21.1–24.2 wt%), Cr (2145–2454 ppm) and Ni (827–1123 ppm) contents, and enrichment of LILE and Th over HFSE and LREE (Nb* = 0.27–0.39). The basalts have SiO_2 = 47.5–50.4 wt%, MgO = 6.7–9.3 wt%, TiO_2 = 0.7–1.1 wt% and CaO = 12.1–13.2 wt%. They show depletion of HFSE over LILE and flat chondrite-normalized REE patterns, with Nb* = 0.35–0.41, Eu* = 0.92–0.96 and $(La/Yb)_n$ = 1.23–1.41. The andesites have SiO_2 = 51.6–55.5 wt%, MgO = 7.7–9.2 wt% ($Mg^{\#}$ = 65–68), Cr = 365–460 ppm and Ni = 46–57 ppm. These characteristics are identical to those of the high-$Mg^{\#}$ andesite, but distinctive from the boninite because of its high TiO_2 contents (0.66–0.76 wt%). The high-$Mg^{\#}$ andesites are characterized by highly enriched LILE, depleted HFSE (Nb* = 0.31–0.33) and relatively fractionated chondrite-normalized REE patterns ($(La/Yb)_{cn}$ = 2.49–2.71). The volcanic rocks have enriched Sr–Nd isotopic compositions, with $(^{87}Sr/^{86}Sr)_i$ = 0.70568–0.71147 and $\varepsilon_{Nd}(t)$ = −1.2 – +2.0 (Fig. 7). These observations indicate that the Jianshui mafic–intermediate rocks were generated in an arc or back-arc setting (Dong & Zhu 1999).

In combination with the coexistence of the N-MORB- and SSZ-type ophiolites, late Paleozoic ultramafic–mafic rocks in the Babu area are genetically related to the Paleotethyan subduction, rather than the Emeishan large igneous province or the Song Da rift.

Comparison with the Jinshajiang–Ailaoshan–Song Ma ophiolites

In addition to the Babu ophiolites, there are the Jinshajiang, Ailaoshan and Song Ma ophiolites between the South China and Indochina blocks (Fig. 1b). The relationship of the Babu ophiolites to these ophiolites is still a pending problem. Interrogations of whole-rock geochemistry, geochronology and lithology allow us to make some petrogenetic comparisons of these ophiolites.

The Jinshajiang–Ailaoshan–Song Ma ophiolites occur as tectonic mélanges composed largely of blocks and lenses of

Downloaded from https://pubs.geoscienceworld.org/jgs/article-pdf/175/4/667/4240757/jgs2017-121.pdf
by Guangzhou Institute of Geochemistry CAS user

(often intensely deformed) serpentinized peridotite, gabbros and dolerites, plagiogranite, (rare) basalt, chert and limestone in a muddy matrix (Wang *et al.* 2000*a*; Yumul *et al.* 2008; Jian *et al.* 2009*a*,*b*; Lai *et al.* 2014*a*), which lack the Penrose-type layered-cake pseudostratigraphy but are similar to many continental margin-type Alpine Tethyan ophiolites (e.g. Montanini *et al.* 2008). These ophiolites share the same rock units with Babu ophiolites. Many previous geochronological studies have been carried out on the gabbro, basalt and plagiogranite from these ophiolites. For example, Jian *et al.* (2009*b*) reported 439 ± 4, 404 ± 3 and 344 ± 3 Ma for amphibolite xenoliths and a cumulate gabbro of the Jinshajiang ophiolites, and 383 ± 4 and 376 ± 4 Ma for the diabase and plagiogranite from the Ailaoshan ophiolites. Jian *et al.* (2008) reported 338 ± 6, 329 ± 7, 320 ± 10 and 285 ± 6 Ma for a cumulate gabbro–anorthosite association, an amphibole gabbro and a trondhjemite vein from the Jinshajiang ophiolites. Zi *et al.* (2012) reported 347 ± 7 and 283 ± 3 Ma for the trondhjemite and tonalite from the Jinshajiang ophiolites. Wang *et al.* (2000*a*) reported 340 ± 3 and 294 ± 3 Ma for the plagiogranites from the Jinshajiang ophiolites, and 362 ± 41 Ma for the plagiogranite from the Ailaoshan ophiolites. Lai *et al.* (2014*a*) reported 365 ± 7, 335 ± 6 and 351 ± 11 Ma for the dolerites from the Ailaoshan ophiolites. Zhang *et al.* (2014) reported 340 ± 29, 280 ± 2 and 315 ± 4 Ma for the pyroxenites and plagioclase–amphibole schists from the Song Ma ophiolites. Vuong *et al.* (2013) reported 387 ± 6, 313 ± 32 and 338 ± 24 Ma for the metagabbros from the Song Ma ophiolites. In summary, the ages of these ophiolites show a wide range from 439 to 280 Ma, which is broadly synchronous with the Babu ophiolites (359–265 Ma).

Geochemically, previous studies subdivided the mafic rocks of the Jinshajiang–Ailaoshan–Song Ma ophiolites into two suites. For example, Xu & Castillo (2004) proposed that the basalts from the Jinshajiang ophiolites show enriched (E)-MORB-type geochemical compositions and the gabbros from the Ailaoshan ophiolites show N-MORB-type. Lai *et al.* (2014*a*) divided the mafic rocks from the Ailaoshan ophiolite into two groups based on fractionation invariant Zr/Nb ratios; namely, suites DC1 and DC2. The oldest age of DC2 tholeiitic basalts may extend into the Devonian and they were likely to have formed early in the development of a volcanic passive margin, and the increased crustal extension led to N-MORB-type DC1 magmas, which may have occurred throughout the Late Devonian to Early Carboniferous. Some serpentinite samples of the Song Ma ophiolites (414 Ma) are highly LREE-enriched (chondrite-normalized) approaching continental rift (broadly OIB) basalt compositions (Trung *et al.* 2006) and the others are geochemically similar to Suite DC2 of the Ailaoshan ophiolite defined by Lai *et al.* (2014*a*). These proposals were redefined by Halpin *et al.* (2016), who classified mafic–ultramafic rocks of the Song Ma ophiolites into the Suites SH-1 (N-MORB-like) and SH-2 (E-MORB-like). These geochemical characteristics resemble the coexistent N-MORB- and SSZ-type Babu ophiolites along the China–Vietnam border. Thus, considering the coincident rock units, geochemical compositions and synchronous ages, the Babu ophiolites may be a part of the Jinshajiang–Ailaoshan–Song Ma ophiolites.

Mid-Neoproterozoic arc magmatism and high-pressure metamorphic rocks in the Shigu, Diancangshan and Ailaoshan complexes indicate that the South China and the Simao–Indochina blocks amalgamated in the Mid-Neoproterozoic following the assemblage of the Rodinia supercontinent (860–730 Ma; Qi *et al.* 2014; Cai *et al.* 2015; Wang *et al.* 2016). After that, the Jinshajiang–Ailaoshan–Song Ma suture zone showed a long period of quiescence. The Panjiazhai OIB-like basalts (Cheng & Shen 1997), Jinshajiang low-Ti continental flood basalt (443–401 Ma; Jian *et al.* 2009*a*) and the changes in sedimentary facies from Silurian–Early Devonian siliciclastic rocks to Late Devonian–Carboniferous pelagic shale–limestone–chert in the Ailaoshan area (Xia *et al.* 2016) suggest that the continental rifting of the Simao–Indochina block from the South China block may have initiated from the Silurian. Recent new zircon U–Pb dating results from the ophiolites along the Jinshajiang–Ailaoshan–Song Ma suture have revealed a multi-stage history of the ocean or back-arc basin opening: nonvolcanic rifting (*c.* 443–401 Ma), resultant sea-floor spreading (*c.* 387–377 Ma), volcanic rifting above an upwelling asthenosphere (*c.* 359–345 Ma), and a late phase of sea-floor spreading (*c.* 346–265 Ma; Jian *et al.* 2009*a*,*b*; Zi *et al.* 2012; Lai *et al.* 2014*a*,*b*; Zhang *et al.* 2014). After reaching its maximum expansion during the Late Carboniferous, the Jinshajiang–Ailaoshan–Song Ma ocean or back-arc basin may have commenced its closure by westward subduction beneath the Simao–Indochina block, and generated the Late Carboniferous–Permian Jomda–Weixi (Yang *et al.* 2014), Wusu–Yaxuanqiao (Fan *et al.* 2010), Truong Son (Liu *et al.* 2012; Kamvong *et al.* 2014; Shi *et al.* 2015), Jianshui (Dong & Zhu 1999) and Cao Bang (Thanh *et al.* 2014; Halpin *et al.* 2016) arc or back-arc basin magmatism in the Jinshajiang, Ailaoshan and Song Ma suture zones.

Conclusions

(1) Detailed geological, geochemical and geochronological investigations suggest the coexistence of N-MORB- and SSZ-type ophiolites (270–265 Ma) in the Babu area (SW China).

(2) The N-MORB-type ophiolites were derived from a depleted mantle source and the SSZ-type ophiolites were derived from an enriched mantle source metasomatized by subducted oceanic sediment- or slab-derived melt or fluid.

(3) The coexistent N-MORB- and SSZ-type ophiolites and other reported late Paleozoic ultramafic–mafic rocks in the Babu area are genetically related to the Paleotethyan subduction, rather than the Emeishan mantle plume.

(4) Babu ophiolites show similar geochemical and geochronological characteristics to the Jinshajiang–Ailaoshan–Song Ma ophiolites and were parts of those ophiolites.

Acknowledgements We are grateful to Subject Editor L. A. Kirstein, ande Ş. Altunkaynak and H. Furnes for their constructive and helpful reviews. We would like to thank X.-P. Xia, Y.-F. Cai and L.-Y. Ma for their help in fieldwork and zircon U–Pb analyses.

Funding This study is financially supported by the National Science Foundation of China (41502210 and 41190073), the National Basic Research Program of China (2014CB440901) and the Fundamental Research Funds for the Central Universities to Sun Yat-Sen University.

Scientific editing by Linda Kirstein

References

Balykin, P.A., Polyakov, G.V., Izokh, A.E., Tran, T.H., Ngo, T.P., Tran, Q.H. & Petrova, T.E. 2010. Geochemistry and petrogenesis of Permian ultramafic–mafic complexes of the Jinping–Song Da rift (southeastern Asia). *Russian Geology and Geophysics*, **51**, 611–624.

Belousova, E.A., Jimenez, J.M.G. *et al.* 2015. The enigma of crustal zircons in upper-mantle rocks: Clues from the Tumut ophiolite, southeast Australia. *Geology*, **43**, 119–122.

Burton, K.W., Schiano, P., Birck, J.L. & Allègre, C.J. 1999. Osmium isotope disequilibrium between mantle minerals in a spinel-lherzolite. *Earth and Planetary Science Letters*, **172**, 311–322.

Cai, J.X. & Zhang, K.J. 2009. A new model for the Indochina and South China collision during the Late Permian to the Middle Triassic. *Tectonophysics*, **467**, 35–43.

Cai, Y.F., Wang, Y.J., Cawood, P.A., Fan, W.M., Liu, H.C., Xing, X.W. & Zhang, Y.Z. 2014. Neoproterozoic subduction along the Ailaoshan zone, South China: Geochronological and geochemical evidence from amphibolite. *Precambrian Research*, **245**, 13–28.

Cai, Y.F., Wang, Y.J., Cawood, P.A., Zhang, Y.Z. & Zhang, A.M. 2015. Neoproterozoic crustal growth of the Southern Yangtze Block: Geochemical

Downloaded from https://pubs.geoscienceworld.org/jgs/article-pdf/175/4/667/4240757/jgs2017-121.pdf
by Guangzhou Institute of Geochemistry CAS user

and zircon U–Pb geochronological and Lu–Hf isotopic evidence of Neoproterozoic diorite from the Ailaoshan zone. *Precambrian Research*, **266**, 137–149.
Cawood, P.A., Wang, Y.J., Xu, Y.J. & Zhao, G.C. 2013. Locating South China in Rodinia and Gondwana: A fragment of greater India lithosphere? *Geology*, **41**, 903–906.
Cheng, H.L. & Shen, S.Y. 1997. Metamorphic Basalts in Panjiazhai, Ailao Mountain Area, Yunnan. *Tethyan Geology*, **21**, 62–72 [in Chinese with English abstract].
Deng, J., Wang, Q.F., Li, G.J., Li, C.S. & Wang, C.M. 2014*a*. Tethys tectonic evolution and its bearing on the distribution of important mineral deposits in the Sanjiang region, SW China. *Gondwana Research*, **26**, 419–437.
Deng, J., Wang, Q.F., Li, G.J. & Santosh, M. 2014*b*. Cenozoic tectono-magmatic and metallogenic processes in the Sanjiang region, southwestern China. *Earth-Science Reviews*, **138**, 268–299.
Dilek, Y. & Furnes, H. 2011. Ophiolite genesis and global tectonics: Geochemical and tectonic fingerprinting of ancient oceanic lithosphere. *Geological Society of America Bulletin*, **123**, 387–411.
Dilek, Y. & Furnes, H. 2014. Ophiolites and their origins. *Elements*, **10**, 93–100.
Dilek, Y., Furnes, H. & Shallo, M. 2008. Geochemistry of the Jurassic Mirdita Ophiolite (Albania) and the MORB to SSZ evolution of a marginal basin oceanic crust. *Lithos*, **100**, 174–209.
Dong, Y.P. & Zhu, B.Q. 1999. Geochemical characteristics of the arc basalts in Jianshui area (SE Yunnan province) and its tectonic implication for the Paleotethyan evolution in SW China. *Chinese Science Bulletin*, **44**, 2323–2327 [in Chinese].
Du, Y.S., Yang, J.H. & Huang, H. 2014. *Hercynian–Indonisian Sedimentary Geology of Youjiang Orogenic Belt*. China University of Geosciences Press, Wuhan [in Chinese].
Fan, W.M., Zhang, C.H., Wang, Y.J., Guo, F. & Peng, T.P. 2008. Geochronology and geochemistry of Permian basalts in western Guangxi Province, Southwest China: Evidence for plume–lithosphere interaction. *Lithos*, **102**, 218–236.
Fan, W.M., Wang, Y.J., Zhang, A.M., Zhang, F.F. & Zhang, Y.Z. 2010. Permian arc–back-arc basin development along the Ailaoshan tectonic zone: Geochemical, isotopic and geochronological evidence from the Mojiang volcanic rocks, Southwest China. *Lithos*, **119**, 553–568.
Faure, M., Lepvrier, C., Nguyen, V.V., Vu, T.V., Lin, W. & Chen, Z. 2014. The South China block–Indochina collision: Where, when, and how? *Journal of Asian Earth Sciences*, **79**, 260–274.
Feng, Q.L. & Liu, B.P. 2002. Early Permian Radiolarians from Babu Ophiolitic Mélange in Southeastern Yunnan. *Earth Science – Journal of China University of Geosciences*, **27**, 1–5 [in Chinese with English abstract].
Furnes, H. & Dilek, Y. 2017. Geochemical characterization and petrogenesis of intermediate to silicic rocks in ophiolites: A global synthesis. *Earth-Science Reviews*, **166**, 1–37.
Furnes, H., de Wit, M. & Dilek, Y. 2014. Four billion years of ophiolites reveal secular trends in oceanic crust formation. *Geoscience Frontiers*, **5**, 571–603.
Furnes, H., Dilek, Y. & de Wit, M. 2015. Precambrian greenstone sequences represent different ophiolite types. *Gondwana Research*, **27**, 649–685.
Gao, S., Rudnick, R.L., Carlson, R.W., McDonough, W.F. & Liu, Y.S. 2002. Re–Os evidence for replacement of ancient mantle lithosphere beneath the North China craton. *Earth and Planetary Science Letters*, **198**, 307–322.
Glotov, A.I., Polyakov, G.V. *et al.* 2001. The Ban Phuc Ni–Cu–PGE deposit related to the Phanerozoic komatiite–basalt association in the Song Da Rift, nortwestern Vietnam. *Canadian Mineralogist*, **39**, 573–589.
Halpin, A.J., Tran, T.H., Lai, C.K., Meffre, S., Crawford, A.J. & Zaw, K. 2016. U–Pb zircon geochronology and geochemistry from NE Vietnam: A 'tectonically disputed' territory between the Indochina and South China blocks. *Gondwana Research*, **34**, 254–273.
Hanchar, J.M. & Watson, E.B. 2003. Zircon saturation thermometry. *In*: Hanchar, J.M. & Hoskin, P.W.O. (eds) *Zircon*. Mineralogical Society of America and Geochemical Society, Reviews in Mineralogy and Geochemistry, **53**, 89–112.
Hanski, E., Kamenetsky, V.S., Luo, Z.Y., Xu, Y.G. & Kuzmin, D.V. 2010. Primitive magmas in the Emeishan Large Igneous Province, southwestern China and northern Vietnam. *Lithos*, **119**, 75–90.
Hara, H., Kunii, M. *et al.* 2012. Petrography and geochemistry of clastic rocks within the Inthanon zone, northern Thailand: Implications for Paleo-Tethys subduction and convergence. *Journal of Asian Earth Sciences*, **61**, 2–15.
Hawkesworth, C.J., Turner, S., Peate, W.D. & Calsteren, P.V. 1997. Elemental U and Th variations in island arc rocks: Implications for U-series isotopes. *Chemical Geology*, **139**, 207–221.
Hoa, T.T., Anh, T.T. *et al.* 2008*a*. Permo-Triassic intermediate–felsic magmatism of the Truong Son belt, eastern margin of Indochina. *Comptes Rendus Géoscience*, **340**, 112–126.
Hoa, T.T., Izokh, A.E. *et al.* 2008*b*. Permo-Triassic magmatism and metallogeny of Northern Vietnam in relation to the Emeishan plume. *Russian Geology and Geophysics*, **49**, 480–491.
Huang, H., Du, Y.S., Yang, J.H., Zhou, L., Hu, L.S., Huang, H.W. & Huang, Z.Q. 2014. Origin of Permian basalts and clastic rocks in Napo, Southwest China: Implications for the erosion and eruption of the Emeishan large igneous province. *Lithos*, **208**, 324–338.
Jian, P., Liu, D.Y. & Sun, X.M. 2008. SHRIMP dating of the Permo-Carboniferous Jinshajiang ophiolite, southwestern China: Geochronological constraints for the evolution of Paleo-Tethys. *Journal of Asian Earth Sciences*, **32**, 371–384.
Jian, P., Liu, D.Y., Kroner, A., Zhang, Q., Wang, Y.Z., Sun, X.M. & Zhang, W. 2009*a*. Devonian to Permian plate tectonic cycle of the Paleo-Tethys Orogen in southwest China (I): Geochemistry of ophiolites, arc/back-arc assemblages and within-plate igneous rocks. *Lithos*, **113**, 748–766.
Jian, P., Liu, D.Y., Kroner, A., Zhang, Q., Wang, Y.Z., Sun, X.M. & Zhang, W. 2009*b*. Devonian to Permian plate tectonic cycle of the Paleo-Tethys Orogen in southwest China (II): Insights from zircon ages of ophiolites, arc/back-arc assemblages and within-plate igneous rocks and generation of the Emeishan CFB province. *Lithos*, **113**, 767–784.
Kamvong, T., Zaw, K., Meffre, S., Maas, R., Stein, H. & Lai, C.K. 2014. Adakites in the Truong Son and Loei fold belts, Thailand and Laos: Genesis and implications for geodynamics and metallogeny. *Gondwana Research*, **26**, 165–184.
Lai, C.K., Meffre, S., Crawford, A.J., Zaw, K., Halpin, J.A., Xue, C.D. & Salam, A. 2014*a*. The Central Ailaoshan ophiolite and modern analogs. *Gondwana Research*, **26**, 75–88.
Lai, C.K., Meffre, S., Crawford, A.J., Zaw, K., Xue, C.D. & Halpin, J.A. 2014*b*. The Western Ailaoshan Volcanic Belts and their SE Asia connection: A new tectonic model for the Eastern Indochina Block. *Gondwana Research*, **26**, 52–74.
Lan, C.Y., Chung, S.L., Van Long, T., Lo, C.H., Lee, T.Y., Mertzman, S.A. & Shen, J.J.S. 2003. Geochemical and Sr–Nd isotopic constraints from the Kontum massif, central Vietnam on the crustal evolution of the Indochina block. *Precambrian Research*, **122**, 7–27.
Le Bas, M.J., Le Maitre, R.W., Streckeisen, A. & Zanettin, B. 1986. A chemical classification of volcanic rocks based on the total alkali–silica diagram. *Journal of Petrology*, **27**, 745–750.
Lepvrier, C., Maluski, H., Van Tich, V., Leyreloup, A., Thi, P.T. & Van Vuong, N. 2004. The Early Triassic Indosinian orogeny in Vietnam (Truong Son Belt and Kontum Massif); implications for the geodynamic evolution of Indochina. *Tectonophysics*, **393**, 87–118.
Lepvrier, C., Van, V.N., Maluski, H., Thi, P.T. & Van, V.T. 2008. Indosinian tectonics in Vietnam. *Comptes Rendus Géoscience*, **340**, 94–111.
Li, C.S., Ripley, E.M., Tao, Y. & Hu, R.Z. 2016. The significance of PGE variations with Sr–Nd isotopes and lithophile elements in the Emeishan flood basalt province from SW China to northern Vietnam. *Lithos*, **248**, 1–11.
Litvak, V.D. & Poma, S. 2010. Geochemistry of mafic Paleocene volcanic rocks in the Valle del Cura region: Implications for the petrogenesis of primary mantle-derived melts over the Pampean flat-slab. *Journal of South American Earth Sciences*, **29**, 705–716.
Liu, H.C., Wang, Y.J., Fan, W.M., Zi, J.W., Cai, Y.F. & Yang, G.L. 2014. Petrogenesis and tectonic implications of Late-Triassic high εNd(t)–εHf(t) granites in the Ailaoshan tectonic zone (SW China). *Science China – Earth Sciences*, **57**, 2181–2194.
Liu, H.C., Wang, Y.J., Cawood, P.A., Fan, W.M., Cai, Y.F. & Xing, X.W. 2015. Record of Tethyan ocean closure and Indosinian collision along the Ailaoshan suture zone (SW China). *Gondwana Research*, **27**, 1292–1306.
Liu, H.C., Wang, Y.J., Guo, X.F., Fan, W.M. & Song, J.J. 2017*a*. Late Triassic post-collisional slab break-off along the Ailaoshan suture: insights from OIB-like metagabbros and associated rocks. *International Journal of Earth Sciences*, **106**, 1359–1373.
Liu, H.C., Wang, Y.J. & Zi, J.W. 2017*b*. Petrogenesis of the Dalongkai mafic–ultramafic intrusion and its tectonic implication for the Paleotethyan evolution in the Ailaoshan tectonic zone (SW China). *Journal of Asian Earth Sciences*, **141**, 112–124.
Liu, J.L., Tran, M.D. *et al.* 2012. Permo-Triassic granitoids in the northern part of the Truong Son belt, NW Vietnam: Geochronology, geochemistry and tectonic implications. *Gondwana Research*, **22**, 628–644.
Luck, J.M. & Allègre, C.J. 1991. Osmium isotopes in ophiolites. *Earth and Planetary Science Letters*, **107**, 406–415.
Macpherson, C.G. & Hall, R. 2001. Tectonic setting of Eocene boninite magmatism in the Izu–Bonin–Mariana forearc. *Earth and Planetary Science Letters*, **186**, 215–230.
Metcalfe, I. 2002. Permian tectonic framework and palaeogeography of SE Asia. *Journal of Asian Earth Sciences*, **20**, 551–566.
Metcalfe, I. 2006. Paleozoic and Mesozoic tectonic evolution and palaeogeography of East Asian crustal fragments: The Korean Peninsula in context. *Gondwana Research*, **9**, 24–46.
Metcalfe, I. 2011. Tectonic framework and Phanerozoic evolution of Sundaland. *Gondwana Research*, **19**, 3–21.
Miyashiro, A. 1974. Volcanic rock series in island arcs and active continental margins. *American Journal of Science*, **274**, 321–355.
Montanini, A., Tribuzio, R. & Vernia, L. 2008. Petrogenesis of basalts and gabbros transition (External Liguride from an ancient continent–ocean ophiolites, Northern Italy). *Lithos*, **101**, 453–479.
Nam, T.N., Toriumi, M., Sano, Y., Terada, K. & Thang, T.T. 2003. 2.9, 2.36, and 1.96 Ga zircons in orthogneiss south of the Red River shear zone in Viet Nam: evidence from SHRIMP U–Pb dating and tectonothermal implications. *Journal of Asian Earth Sciences*, **21**, 743–753.
Ngo, T.X., Santosh, M., Tran, H.T. & Pham, H.T. 2016. Subduction initiation of Indochina and South China blocks: insight from the forearc ophiolitic peridotites of the Song Ma Suture Zone in Vietnam. *Geological Journal*, **51**, 421–442.
Pearce, J.A. 2003. Quantifying element transfer from slab to mantle at subduction zones. *Geochimica et Cosmochimica Acta*, **67**, A377.

Downloaded from https://pubs.geoscienceworld.org/jgs/article-pdf/175/4/667/4240757/jgs2017-121.pdf
by Guangzhou Institute of Geochemistry CAS user

Pearce, J.A. 2014. Immobile element fingerprinting of ophiolites. *Elements*, **10**, 101–108.

Polyakov, G.V., Balykin, P.A. *et al.* 1998. Evolution of the Mesozoic–Cenozoic magmatism of the Song Da rift and its contouring structures. *Geologiya i Geofizika*, **39**, 695–706.

Qi, X.X., Santosh, M., Zhu, L.H., Zhao, Y.H., Hu, Z.C., Zhang, C. & Ji, F.B. 2014. Mid-Neoproterozoic arc magmatism in the northeastern margin of the Indochina block, SW China: Geochronological and petrogenetic constraints and implications for Gondwana assembly. *Precambrian Research*, **245**, 207–224.

Roger, F., Jolivet, M. *et al.* 2014. Emplacement and cooling of the Dien Bien Phu granitic complex: Implications for the tectonic evolution of the Dien Bien Phu Fault (Truong Son Belt, NW Vietnam). *Gondwana Research*, **26**, 785–801.

Roy-Barman, M., Luck, J.M. & Allègre, C.J. 1996. Os isotopes in orogenic lherzolite massifs and mantle heterogeneities. *Chemical Geology*, **130**, 55–64.

Saal, A.E., Takazawa, E., Frey, F.A., Shimizu, N. & Hart, S.R. 2001. Re–Os isotopes in the Horoman peridotite: Evidence for refertilization? *Journal of Petrology*, **42**, 25–37.

Saccani, E. 2015. A new method of discriminating different types of post-Archean ophiolitic basalts and their tectonic significance using Th–Nb and Ce–Dy–Yb systematics. *Geoscience Frontiers*, **6**, 481–501.

Sengor, A.M.C. & Hsu, K.J. 1984. The Cimmerides of Eastern Asia: history of the eastern end of the Paleo-Tethys. *Mémoire de la Société Géologique de France*, **147**, 139–167.

Shi, G.Y., Sun, X.M., Pan, W.J., Hu, B.M., Qu, W.J., Du, A.D. & Li, C. 2012*a*. Re–Os dating of auriferous pyrite from the Zhenyuan super-large gold deposit in Ailaoshan gold belt, Yunnan Province, Southwestern China. *Chinese Science Bulletin*, **57**, 4578–4586.

Shi, M.F., Lin, F.C. *et al.* 2015. Zircon U–Pb ages and geochemistry of granitoids in the Truong Son terrane, Vietnam: Tectonic and metallogenic implications. *Journal of Asian Earth Sciences*, **101**, 101–120.

Shi, R.D., Zhi, X.C., Lei, C. & Ding, B.H. 2006. Comments on the progress on the applications of Re–Os isotopic study on the ophiolites. *Acta Petrologica Sinica*, **22**, 1685–1695.

Shi, R.D., Griffin, W.L. *et al.* 2012*b*. Melt/mantle mixing produces podiform chromite deposits in ophiolites: Implications of Re–Os systematics in the Dongqiao Neo-Tethyan ophiolite, northern Tibet. *Gondwana Research*, **21**, 194–206.

Shinjo, R., Meshesha, D., Orihashi, Y., Haraguchi, S. & Tamaki, K. 2015. Sr–Nd–Pb–Hf isotopic constraints on the diversity of magma sources beneath the Aden Ridge (central Gulf of Aden) and plume–ridge interaction. *Journal of Mineralogical and Petrological Sciences*, **110**, 97–110.

Shirey, S.B. & Walker, R.J. 1998. The Re–Os isotope system in cosmochemistry and high-temperature geochemistry. *Annual Review of Earth and Planetary Sciences*, **26**, 423–500.

Sone, M. & Metcalfe, I. 2008. Parallel Tethyan sutures in mainland Southeast Asia: New insights for Palaeo-Tethys closure and implications for the Indosinian orogeny. *Comptes Rendus Géoscience*, **340**, 166–179.

Sun, S.S. & McDonough, W.F. 1989. Chemical and isotopic systematics of oceanic basalts: implication for mantle composition and process. *In*: Saunders, A.D. & Norry, M.J. (eds) *Magmatism in the Ocean Basins*. Geological Society, London, Special Publications, **42**, 313–345, https://doi.org/10.1144/GSL.SP.1989.042.01.19

Thanh, N.X., Hai, T.T., Hoang, N., Lan, V.Q., Kwon, S., Itaya, T. & Santosh, M. 2014. Backarc mafic–ultramafic magmatism in Northeastern Vietnam and its regional tectonic significance. *Journal of Asian Earth Sciences*, **90**, 45–60.

Tran, T.H., Lan, C.Y. *et al.* 2015. Petrogenesis of Late Permian silicic rocks of Tu Le basin and Phan Si Pan uplift (NW Vietnam) and their association with the Emeishan large igneous province. *Journal of Asian Earth Sciences*, **109**, 1–19.

Trung, N.M., Tsujimori, T. & Itaya, T. 2006. Honvang serpentinite body of the Song Ma fault zone, Northern Vietnam: A remnant of oceanic lithosphere within the Indochina–South China suture. *Gondwana Research*, **9**, 225–230.

Usuki, T., Lan, C.Y., Wang, K.L. & Chiu, H.Y. 2013. Linking the Indochina block and Gondwana during the Early Paleozoic: Evidence from U–Pb ages and Hf isotopes of detrital zircons. *Tectonophysics*, **586**, 145–159.

Uysal, I., Ersoy, E.Y. *et al.* 2012. Coexistence of abyssal and ultra-depleted SSZ type mantle peridotites in a Neo-Tethyan Ophiolite in SW Turkey: Constraints from mineral composition, whole-rock geochemistry (major–trace–REE–PGE), and Re–Os isotope systematics. *Lithos*, **132**, 50–69.

Vuong, N.V., Hansen, B.T., Wemmer, K., Lepvrier, C., Tich, V.V. & Thang, T.T. 2013. U/Pb and Sm/Nd dating on ophiolitic rocks of the Song Ma suture zone (northern Vietnam): Evidence for upper Paleozoic Paleotethyan lithospheric remnants. *Journal of Geodynamics*, **69**, 140–147.

Wang, C.Y., Zhou, M.F. & Qi, L. 2007. Permian flood basalts and mafic intrusions in the Jinping (SW China) Song Da (northern Vietnam) district: Mantle sources, crustal contamination and sulfide segregation. *Chemical Geology*, **243**, 317–343.

Wang, C.Y., Zhou, M.F., Sun, Y. & Arndt, N.T. 2012. Differentiation, crustal contamination and emplacement of magmas in the formation of the Nantianwan mafic intrusion of the ∼260 Ma Emeishan large igneous province, SW China. *Contributions to Mineralogy and Petrology*, **164**, 281–301.

Wang, Q.F., Deng, J., Li, C.S., Li, G.J., Yu, L. & Qiao, L. 2014*b*. The boundary between the Simao and Yangtze blocks and their locations in Gondwana and Rodinia: Constraints from detrital and inherited zircons. *Gondwana Research*, **26**, 438–448.

Wang, X.F., Metcalfe, I., Jian, P., He, L.Q. & Wang, C.S. 2000*a*. The Jinshajiang–Ailaoshan Suture Zone, China: tectonostratigraphy, age and evolution. *Journal of Asian Earth Sciences*, **18**, 675–690.

Wang, X.F., Metcalfe, I., Jian, P., He, L.Q. & Wang, C.S. 2000*b*. The Jinshajiang suture zone: tectono-stratigraphic subdivision and revision of age. *Science China – Earth Sciences*, **43**, 10–22.

Wang, Y.J., Fan, W.M., Zhang, G.W. & Zhang, Y.H. 2013. Phanerozoic tectonics of the South China Block: Key observations and controversies. *Gondwana Research*, **23**, 1273–1305.

Wang, Y.J., Zhou, Y.Z., Liu, H.C. & Cai, Y.F. 2016. Neoproterozoic subduction along the SW Yangtze Block: Geochronological and geochemical evidence from the Ailaoshan granitic and migmatite rocks. *Precambrian Research*, **2016**, 106–124.

Whattam, S.A., Malpas, J., Smith, I.E.M. & Ali, J.R. 2006. Link between SSZ ophiolite formation, emplacement and arc inception, Northland, New Zealand: U–Pb SHRIMP constraints; Cenozoic SW Pacific tectonic implications. *Earth and Planetary Science Letters*, **250**, 606–632.

Wu, Y.B. & Zheng, Y.F. 2004 Genesis of zircon and its constraints on interpretation of U-Pb age. *Chinese Science Bulletin*, **49**, 1554–1569.

Wu, G.Y., Zhong, D.L., Zhang, Q. & Ji, J.Q. 1999. Babu–Phu Ngu ophiolites: a geological record of Paleotethyan Ocean bordering China and Vietnam. *Gondwana Research*, **2**, 554–557.

Xia, X.P., Nie, X.S., Wang, Y.J., Lai, C.K., Long, X.P. & Meffre, S. 2016. Where was the Ailaoshan Ocean and when did it open: A perspective based on detrital zircon U–Pb age and Hf isotope evidence. *Gondwana Research*, **36**, 488–502.

Xie, J. 2002. *Geochemical Characteristics of the Paleozoic Volcanic Rocks in the Jinshajiang Zone, NW Yunnan and Janshui, SE Yunnan, and Evolution of Paleo-Tethys*. Master's degree thesis, University of Chinese Academy of Sciences, Beijing.

Xu, J.F. & Castillo, P.R. 2004. Geochemical and Nd–Pb isotopic characteristics of the Tethyan asthenosphere: implications for the origin of the Indian Ocean mantle domain. *Tectonophysics*, **393**, 9–27.

Xu, W., Liu, Y.P., Guo, L.G., Ye, L., Pi, D.H. & Liao, Z. 2008*a*. Geochemistry and tectonic setting of the Babu ophiolite in Southeast Yunnan (China). *Acta Mineralogica Sinica*, **28**, 6–14 [in Chinese with English abstract].

Xu, Y.G., Chung, S.L., Jahn, B.M. & Wu, G.Y. 2001. Petrologic and geochemical constraints on the petrogenesis of Permian–Triassic Emeishan flood basalts in southwestern China. *Lithos*, **58**, 145–168.

Xu, Y.G., Luo, Z.Y., Huang, X.L., He, B., Xiao, L., Xie, L.W. & Shi, Y.R. 2008*b*. Zircon U–Pb and Hf isotope constraints on crustal melting associated with the Emeishan mantle plume. *Geochimica et Cosmochimica Acta*, **72**, 3084–3104.

Yang, T.N., Ding, Y., Zhang, H.R., Fan, J.W., Liang, M.J. & Wang, X.H. 2014. Two-phase subduction and subsequent collision defines the Paleotethyan tectonics of the southeastern Tibetan Plateau: Evidence from zircon U–Pb dating, geochemistry, and structural geology of the Sanjiang orogenic belt, southwest China. *Geological Society of American Bulletin*, **126**, 1654–1682.

Yin, A. & Harrison, T.M. 2000. Geologic evolution of the Himalayan–Tibetan orogen. *Annual Review of Earth and Planetary Sciences*, **28**, 211–280.

Yumul, G.P., Zhou, M.F., Wang, C.Y., Zhao, T.P. & Dimalanta, C.B. 2008. Geology and geochemistry of the Shuanggou ophiolite (Ailao Shan ophiolitic belt), Yunnan Province, SW China: Evidence for a slow-spreading oceanic basin origin. *Journal of Asian Earth Sciences*, **32**, 385–395.

Yunnan BGMR. 1990. *Regional Geology of Yunnan Province*. Geology Publishing House, Beijing, 273–428 [in Chinese].

Zaw, K., Meffre, S. *et al.* 2014. Tectonics and metallogeny of mainland Southeast Asia – A review and contribution. *Gondwana Research*, **26**, 5–30.

Zhang, B.H., Ding, J., Zhang, L.K., Zhang, B. & Chen, M.H. 2013*a*. SHRIMP Zircon U–Pb Chronology of the Babu Ophiolite in Southeastern Yunnan Province (China). *Acta Geologica Sinica*, **87**, 1498–1509 [in Chinese with English abstract].

Zhang, Q., Wang, C.Y., Liu, D., Jian, P., Qian, Q., Zhou, G.Q. & Robinson, P.T. 2008. A brief review of ophiolites in China. *Journal of Asian Earth Sciences*, **32**, 308–324.

Zhang, R.Y., Lo, C.H. *et al.* 2013*b*. Origin and tectonic implication of ophiolite and eclogite in the Song Ma Suture Zone between the South China and Indochina Blocks. *Journal of Metamorphic Geology*, **31**, 49–62.

Zhang, R.Y., Lo, C.H., Li, X.H., Chung, S.L., Anh, T.T. & Tri, T.T. 2014. U–Pb dating and tectonic implication of ophiolite and metabasite from the Song Ma suture zone, northern Vietnam. *American Journal of Science*, **314**, 649–678.

Zhang, X.Z., Dong, Y.S. *et al.* 2016. Carboniferous and Permian evolutionary records for the Paleo-Tethys Ocean constrained by newly discovered Xiangtaohu ophiolites from central Qiangtang, central Tibet. *Tectonics*, **35**, 1670–1686.

Zhang, Z.C., Mahoney, J.J., Mao, J.W. & Wang, F.H. 2006. Geochemistry of picritic and associated basalt flows of the western Emeishan flood basalt province, China. *Journal of Petrology*, **47**, 1997–2019.

Zhong, D.L. 1998. *The Paleotethysides in West Yunnan and Sichuan*. Science Press, Beijing [in Chinese].

Zhou, M.F., Zhao, J.H., Qi, L., Su, W.C. & Hu, R.Z. 2006. Zircon U–Pb geochronology and elemental and Sr–Nd isotope geochemistry of Permian mafic rocks in the Funing area, SW China. *Contributions to Mineralogy and Petrology*, **151**, 1–19.

Downloaded from https://pubs.geoscienceworld.org/jgs/article-pdf/175/4/667/4240757/jgs2017-121.pdf
by Guangzhou Institute of Geochemistry CAS user

Zhu, J.J., Hu, R.Z., Bi, X.W., Zhong, H. & Chen, H. 2011. Zircon U–Pb ages, Hf–O isotopes and whole-rock Sr–Nd–Pb isotopic geochemistry of granitoids in the Jinshajiang suture zone, SW China: Constraints on petrogenesis and tectonic evolution of the Paleo-Tethys Ocean. *Lithos*, **126**, 248–264.

Zi, J.W., Cawood, P.A., Fan, W.M., Wang, Y.J. & Tohver, E. 2012. Contrasting rift and subduction-related plagiogranites in the Jinshajiang ophiolitic mélange, southwest China, and implications for the Paleo-Tethys. *Tectonics*, **31**, 1–18.

Zi, J.W., Cawood, P.A., Fan, W.M., Tohver, E., Wang, Y.J., McCuaig, T.C. & Peng, T.P. 2013. Late Permian–Triassic magmatic evolution in the Jinshajiang orogenic belt, SW China and implications for orogenic processes following closure of the Paleo-Tethys. *American Journal of Science*, **313**, 81–112.

Downloaded from https://pubs.geoscienceworld.org/jgs/article-pdf/175/4/667/4240757/jgs2017-121.pdf
by Guangzhou Institute of Geochemistry CAS user